

DYNAMIC BUCKLING OF ELASTIC STRUCTURES:  
CRITERIA AND ESTIMATES

by

Bernard Budiansky

Harvard University, Cambridge, Massachusetts

Distribution of this report is provided in the interest of information exchange. Responsibility for the contents resides in the author or organization that prepared it.

FACILITY FORM 902

N66-22209

(ACCESSION NUMBER)	(THRU)
49	1
(PAGES)	(CODE)
	32
(NASA CR OR TMX OR AD NUMBER)	(CATEGORY)

Report SM-7  
January 1966

GPO PRICE \$ \_\_\_\_\_

CFSTI PRICE(S) \$ \_\_\_\_\_

Hard copy (HC) 2.00

Microfiche (MF) .50

DYNAMIC BUCKLING OF ELASTIC STRUCTURES:  
CRITERIA AND ESTIMATES\*

by

Bernard Budiansky  
Harvard University, Cambridge, Massachusetts

ABSTRACT

The concept of the buckling of an elastic structure subjected to time-dependent loads is examined critically and criteria for dynamic buckling are reviewed and discussed. Attention is restricted to structures that are sensitive to initial imperfections, and hence are prone to catastrophic failures. Generalized estimates are made for the dynamic buckling strengths of such structures subjected to various loading histories.

INTRODUCTION

There have been numerous studies in recent years on dynamic buckling, but this paper does not pretend to survey these developments comprehensively. Rather, attention will be limited to the recapitulation, assessment, and expansion of a general approach to the problem that has been presented earlier (Budiansky and Hutchinson, 1964; Hutchinson and Budiansky, 1966). In this approach only imperfection-sensitive structures that are prone to catastrophic buckling failure are explicitly studied. Analytic specification of such

---

\* Presented at the International Conference on Dynamic Stability of Structures, Northwestern University, October 18-20, 1965.

This work was supported in part by the National Aeronautics and Space Administration under Grant NsG-559, and by the Division of Engineering and Applied Physics, Harvard University.

structures, definitions of dynamic buckling loads, estimates of the loads and qualitative assessments of the accuracy of these estimates are among the topics to be presented.

#### STATIC AND DYNAMIC LOADS

Static buckling of a structure under dead (constant directional) loading can be studied by assuming the application of loads  $\underline{q} = \lambda \underline{q}_0$ , where  $\underline{q}_0$  is fixed, and where the scalar multiplier  $\lambda$  is supposed to increase very slowly from zero. The critical value  $\lambda_S$  of this scalar that causes buckling will be called the static buckling load. Dynamic application of the same distribution of loads  $\underline{q}_0$  will be specified by the time-dependent loading  $\underline{q} = \lambda f(t) \underline{q}_0$ , where the time variation  $f(t)$  is normalized so that its maximum value is unity. Dynamic buckling for a given  $f(t)$  and  $\underline{q}_0$  is studied in the present approach by consideration of the ensemble of structural responses associated with the ensemble of loading histories  $\underline{q} = \lambda f(t) \underline{q}_0$  generated by various values of  $\lambda$ . The critical value of  $\lambda$  that corresponds to dynamic buckling will be called the dynamic buckling load, and designated by  $\lambda_D$ .

Criteria for establishing  $\lambda_S$  as well as  $\lambda_D$  will be described later, but it may be noted now that attention will be restricted to imperfection-sensitive structures, for which both  $\lambda_S$  and  $\lambda_D$  may be greatly influenced by small geometrical imperfections. It will be assumed that the perfect structure has associated with it a classical buckling load  $\lambda_C$  (necessarily bigger than  $\lambda_S$ ) that arises as an eigenvalue in the usual formulation of buckling as an equilibrium-path bifurcation problem. Most of this paper will be devoted to the exploration, for various time-variations  $f(t)$ , of the relations between the three critical loads  $\lambda_S$ ,  $\lambda_C$ , and  $\lambda_D$ .

A brief but general discussion of static buckling, based on the theory of Koiter (1945, 1963), will now be given in order to expose the concept of imperfection-sensitivity, reveal the meaning of the static buckling load  $\lambda_S$ , and lay the foundation for subsequent analyses of dynamic buckling.

### STATIC BUCKLING

#### Field variables and equations

Suppose that under the loading  $\underline{q}$  the elastic structure under consideration acquires displacements  $\underline{u}$ , strains  $\underline{\epsilon}$ , and stresses  $\underline{\sigma}$ . (These field variables are to be interpreted in a generalized sense as entities appropriate to the structure and the theory used in its description. Thus, in a pin-jointed truss,  $\underline{u}$  would represent the set of joint displacements; in a shell  $\underline{\sigma}$  might consist of the distributions of the membrane-stress and bending-moment tensors.) These variables will be required to satisfy the strain-displacement relation

$$\underline{\epsilon} = L_1(\underline{u}) + \frac{1}{2} L_2(\underline{u}) \quad (1)$$

where  $L_1$  and  $L_2$  are linear and quadratic functionals respectively; the stress-strain relation

$$\underline{\sigma} = H(\underline{\epsilon}) \quad (2)$$

where  $H$  is a linear functional; and the variational equation of equilibrium

$$\underline{\sigma} \cdot \delta \underline{\epsilon} = \underline{q} \cdot \delta \underline{u} \quad (3)$$

In Equation (3) the "dot" operation is a shorthand notation that, in a term  $\underline{a} \cdot \underline{b}$ , means the virtual work of stresses (or loads)  $\underline{a}$  acting through strains (or displacements)  $\underline{b}$ , integrated over the whole structure. Thus (3) is a statement of the principle of virtual work and only variations  $\delta \underline{u}$  consistent with boundary conditions on displacement would generally be permitted; the requirement that (3) must hold for all such admissible variations  $\delta \underline{u}$  together

with the strain variation  $\delta \underline{\epsilon}$  that follows from (1) will be considered to guarantee equilibrium of the stresses  $\underline{\sigma}$  and loads  $\underline{q}$ . If the bilinear functional defined by the identity

$$L_2(\underline{u} + \underline{v}) = L_2(\underline{u}) + 2L_{11}(\underline{u}, \underline{v}) + L_2(\underline{v})$$

is introduced, then the strain variation  $\delta \underline{\epsilon}$  compatible with  $\delta \underline{u}$  may be written as

$$\delta \underline{\epsilon} = L_1(\delta \underline{u}) + L_{11}(\underline{u}, \delta \underline{u}) \quad (4)$$

Note that  $L_{11}(\underline{u}, \underline{v}) = L_{11}(\underline{v}, \underline{u})$  and that  $L_{11}(\underline{u}, \underline{u}) = L_2(\underline{u})$ .

It will be convenient to use the additional notation

$$\underline{e} \equiv L_1(\underline{u}) \quad (5)$$

so that

$$\delta \underline{\epsilon} = \delta \underline{e} + L_{11}(\underline{u}, \delta \underline{u}) \quad (6)$$

Finally, the reciprocal relation

$$H(\underline{\epsilon}_1) \cdot \underline{\epsilon}_2 = H(\underline{\epsilon}_2) \cdot \underline{\epsilon}_1 \quad (7)$$

will be assumed valid for all  $\underline{\epsilon}_1$  and  $\underline{\epsilon}_2$ .

#### Perfect structure; prebuckling, buckling, and post-buckling behavior

Apply the external loads  $\underline{q} = \lambda \underline{q}_0$  to the perfect structure; it will be supposed that before buckling occurs the response of the structure is simply

$$\begin{cases} \underline{u} = \lambda \underline{u}_0 \\ \underline{\epsilon} = \lambda \underline{\epsilon}_0 \\ \underline{\sigma} = \lambda \underline{\sigma}_0 \end{cases} \quad (8)$$

where the "trivial" displacement satisfies the condition

$$L_{11}(\underline{u}_0, \underline{v}) = 0 \quad (9)$$

for all  $\underline{v}$ . Thus a linear theory is presumed valid before buckling, with

$\underline{\epsilon}_0 = \underline{e}_0 = L_1(\underline{u}_0)$  ,  $\underline{\sigma}_0 = H(\underline{e}_0)$  , and

$$\underline{\sigma}_0 \cdot \delta \underline{e} = \underline{q}_0 \cdot \delta \underline{u} \quad (10)$$

The occurrence of buckling can be detected by substituting

$$\begin{cases} \underline{u} = \lambda_C \underline{u}_0 + \xi \underline{u}_1 \\ \underline{\epsilon} = \lambda_C \underline{e}_0 + \xi \underline{e}_1 \\ \underline{\sigma} = \lambda_C \underline{\sigma}_0 + \xi \underline{\sigma}_1 \end{cases} \quad (11)$$

into the field equations, linearizing with respect to the scalar  $\xi$  , and simplifying the results by using (9) and (10). Then the eigenvalue problem for the classical buckling load  $\lambda_C$  and the buckling mode  $\underline{u}_1, \underline{e}_1, \underline{\sigma}_1$  is found to be governed by the variational equilibrium equation,

$$\lambda_C \underline{\sigma}_0 \cdot L_{11}(\underline{u}_1, \delta \underline{u}) + \underline{\sigma}_1 \cdot \delta \underline{e} = 0 \quad (12)$$

the strain-displacement relation  $\underline{\epsilon}_1 = \underline{e}_1 = L_1(\underline{u}_1)$  , and the stress-strain relation  $\underline{\sigma}_1 = H(\underline{e}_1)$  . It will be assumed now that only one buckling mode is associated with the lowest eigenvalue  $\lambda_C$  , although the theory can easily be extended to cover the technically important case of multiple buckling modes (Koiter, 1945, 1963; Budiansky and Hutchinson, 1964).

Next, in order to discover how the structure behaves after buckling as  $\lambda$  deviates from  $\lambda_C$  , suppose the magnitude of the eigenfunction  $\underline{u}_1$  to be normalized in some convenient fashion and write

$$\begin{cases} \underline{u} = \lambda \underline{u}_0 + \xi \underline{u}_1 + \xi^2 \underline{u}_2 + \xi^3 \underline{u}_3 + \dots \\ \underline{\epsilon} = \lambda \underline{e}_0 + \xi \underline{e}_1 + \xi^2 \underline{e}_2 + \xi^3 \underline{e}_3 + \dots \\ \underline{\sigma} = \lambda \underline{\sigma}_0 + \xi \underline{\sigma}_1 + \xi^2 \underline{\sigma}_2 + \xi^3 \underline{\sigma}_3 + \dots \end{cases} \quad (13)$$

where  $\underline{u}_2, \underline{u}_3, \dots$  are all orthogonalized to  $\underline{u}_1$  in the sense

$$\underline{\sigma}_0 \cdot L_{11}(\underline{u}_1, \underline{u}_n) = 0 \quad (n=2,3,\dots) \quad (14)$$

Note that (14) also holds for  $n=0$  by virtue of (9), and note also that, as

a consequence of (12), this orthogonality condition implies that

$$\underline{g}_1 \cdot \underline{e}_n = 0 \quad (n \neq 1) \quad (15)$$

which, by (7), implies further that

$$H(\underline{e}_n) \cdot \underline{e}_1 = 0 \quad (n \neq 1) \quad (16)$$

Also, note that from (12), with  $\delta \underline{u} = \underline{u}_1$ ,  $\delta \underline{e} = \underline{e}_1$ ,

$$\underline{g}_0 \cdot L_2(\underline{u}_1) = -\frac{1}{\lambda_C} \underline{g}_1 \cdot \underline{e}_1 \quad (17)$$

Substituting (13) into the equilibrium equation (3), noting that

$$\delta \underline{e} = \delta \underline{e} + \xi L_{11}(\underline{u}_1, \delta \underline{u}) + \xi^2 L_{11}(\underline{u}_2, \delta \underline{u}) + \dots$$

and using (10) and (12) to simplify the result gives

$$\begin{aligned} & \xi \left[ 1 - \frac{\lambda}{\lambda_C} \right] \underline{g}_1 \cdot \delta \underline{e} \\ & + \xi^2 [\lambda \underline{g}_0 \cdot L_{11}(\underline{u}_2, \delta \underline{u}) + \underline{g}_1 \cdot L_{11}(\underline{u}_1, \delta \underline{u}) + \underline{g}_2 \cdot \delta \underline{e}] \\ & + \xi^3 [\lambda \underline{g}_0 \cdot L_{11}(\underline{u}_3, \delta \underline{u}) + \underline{g}_1 \cdot L_{11}(\underline{u}_2, \delta \underline{u}) + \underline{g}_2 \cdot L_{11}(\underline{u}_1, \delta \underline{u}) + \underline{g}_3 \cdot \delta \underline{e}] + \dots = 0 \quad (18) \end{aligned}$$

The choice  $\delta \underline{u} = \underline{u}_1$ ,  $\delta \underline{e} = \underline{e}_1 = \underline{e}_1$  in (18), together with the use of the orthogonality relations (14) and (15) gives

$$\xi \left[ 1 - \frac{\lambda}{\lambda_C} \right] \underline{g}_1 \cdot \underline{e}_1 + \xi^2 \left[ \frac{3}{2} \underline{g}_1 \cdot L_2(\underline{u}_1) \right] + \xi^3 [2 \underline{g}_1 \cdot L_{11}(\underline{u}_1, \underline{u}_2) + \underline{g}_2 \cdot L_2(\underline{u}_1)] + \dots = 0 \quad (19)$$

This result provides the desired information concerning the post-buckling variation of  $\xi$  with  $\lambda$ ; thus, after buckling,

$$\frac{\lambda}{\lambda_C} = 1 + a\xi + b\xi^2 + \dots \quad (20)$$

where

$$a = \frac{\frac{3}{2} \underline{g}_1 \cdot L_2(\underline{u}_1)}{\underline{g}_1 \cdot \underline{e}_1} \quad (21)$$

and

$$b = \frac{2\sigma_1 \cdot L_{11}(u_1, u_2) + \sigma_2 \cdot L_2(u_1)}{\sigma_1 \cdot \epsilon_1} \quad (22)$$

(The functions  $u_2$  and  $\sigma_2$  needed in the evaluation of  $b$ , together with the strain function  $\epsilon_2$ , satisfy the strain-displacement and stress-strain relations

$$\epsilon_2 = L_1(u_2) + \frac{1}{2} L_2(u_1)$$

$$\sigma_2 = H(\epsilon_2)$$

and, from (18), with  $\delta u$  chosen orthogonal to  $u_1$  in the sense of (14), (15), the variational equation of equilibrium

$$\lambda \sigma_0 \cdot L_{11}(u_2, \delta u) + \sigma_2 \cdot \delta \epsilon + \sigma_1 \cdot L_{11}(u_1, \delta u) = 0 \quad .)$$

The variation of  $\lambda/\lambda_C$  with  $\xi$  immediately after buckling is shown by the solid curves in Figure 1 for the three cases  $a \neq 0$ ;  $a = 0$ ,  $b > 0$ ; and  $a = 0$ ,  $b < 0$ . It will now be shown that imperfection sensitivity is associated with only the first and last of these cases.

#### Imperfect structures and imperfection sensitivity

To study the influence of initial imperfections, imagine an initial displacement  $\bar{u}$  to exist in the unloaded, stress-free structure, and redefine the strain  $\epsilon$  in terms of the additional displacement  $u$  as

$$\begin{aligned} \epsilon &= [L_1(u + \bar{u}) + \frac{1}{2} L_2(u + \bar{u})] - [L_1(\bar{u}) + \frac{1}{2} L_2(\bar{u})] \\ &= L_1(u) + \frac{1}{2} L_2(u) + L_{11}(u, \bar{u}) \end{aligned}$$

but continue to impose the stress-strain relation (2) and the equation of equilibrium (3). An approximate solution is effected by using the solution (13) for the perfect case in a Galerkin-type solution of (3), with  $\delta u = u_1 \delta \xi$  and  $\delta \epsilon = [\epsilon_1 + L_{11}(u, u_1) + L_{11}(\bar{u}, u_1)] \delta \xi$ ; this gives



$$(1-\lambda/\lambda_C)\xi + a\xi^2 + b\xi^3 + \dots = - \frac{\sigma \cdot L_{11}(\bar{u}, u_1)}{\sigma_1 \cdot \xi_1}$$

Now let  $\bar{u} = \bar{\xi} u_1$ , and keep only the lowest order term in  $\bar{\xi}$  to get

$$(1-\lambda/\lambda_C)\xi + a\xi^2 + b\xi^3 + \dots = \frac{\lambda}{\lambda_C} \bar{\xi} \quad (23)$$

as the modification of (20) that accounts for an initial imperfection in the shape of the buckling mode. The dotted curves in Figure 1 are based on Equation (23), and illustrate how small values of  $\bar{\xi}$  provide singular perturbations to the relations connecting  $\lambda$  and  $\xi$  in the perfect case. It is seen that in the cases  $a\bar{\xi} < 0$  and  $a = 0, b < 0$  there exist load maxima in the variations of  $\lambda$  with  $\xi$ . Under monotonically increasing loading sharp snap-buckling may be expected at these critical values  $\lambda_S$ , which are less than  $\lambda_C$ ; thus, with respect to buckling, the structure is considered to be imperfection-sensitive for  $a \neq 0$ , and for  $b < 0$ , if  $a = 0$ . The relations between  $\lambda_S$  and  $\lambda_C$  may be estimated for these two cases if  $\bar{\xi}$  is assumed sufficiently small. If terms of degree higher than quadratic in  $\xi$  are neglected in (23) it is easily found by maximizing  $\lambda$  that

$$\left(1 - \frac{\lambda_S}{\lambda_C}\right)^2 + 4a\bar{\xi} \left(\frac{\lambda_S}{\lambda_C}\right) = 0 \quad (24)$$

for  $a\bar{\xi} < 0$ . If, however,  $a = 0$ , then keeping terms of third degree in (23) leads to

$$\left(1 - \frac{\lambda_S}{\lambda_C}\right)^{3/2} - \frac{3\sqrt{3}}{2} \sqrt{-b} |\bar{\xi}| \left(\frac{\lambda_S}{\lambda_C}\right) = 0 \quad (25)$$

for  $b < 0$ . It will be convenient, henceforth, to refer to "quadratic structures" and "cubic structures" as those governed by the cases (i)  $a \neq 0$  and (ii)  $a = 0, b \neq 0$ , respectively. Note, then, that for quadratic

structures  $1 - \frac{\lambda_S}{\lambda_C} = O(|\bar{\xi}|^2)$ , whereas in imperfection-sensitive cubic structures  $1 - \frac{\lambda_S}{\lambda_C} = O(\xi^{2/3})$ ; thus, roughly speaking, "small" imperfections make "large" changes in the buckling load.

The above results for static buckling are essentially contained in Koiter's work; now dynamic considerations will be introduced.

### SINGLE-MODE ANALYSES OF DYNAMIC BUCKLING

#### Modified equilibrium equation; Galerkin solution

To account for inertial forces, it will be assumed that the variational equation of equilibrium (3) may generally be replaced by

$$\underline{g} \cdot \delta \underline{\epsilon} = \underline{q} \cdot \delta \underline{u} - M(\underline{\ddot{u}}) \cdot \delta \underline{u} \quad (26)$$

wherein dots represent differentiation with respect to time, and the factor  $-M(\underline{\ddot{u}})$ , linear in  $\underline{\ddot{u}}$ , represents the inertial loading associated with acceleration. It will be supposed that the reciprocal relation  $M(\underline{u}) \cdot \underline{v} = M(\underline{v}) \cdot \underline{u}$  is valid.

Considering first the imperfect quadratic structure under the loading  $\underline{q} = \lambda f(t) \underline{q}_0$ , seek an approximate solution of (26) in the form

$$\underline{u} = \lambda f(t) \underline{u}_0 + \xi(t) \underline{u}_1 \quad (27)$$

If the inertial forces associated with the prebuckling displacements are neglected -- that is, if  $M(\underline{u}_0)$  is set equal to zero -- it is found that repetition of the Galerkin solution that led to (23) now gives

$$\left( \frac{1}{\omega_1^2} \right) \ddot{\xi} + \left[ 1 - \frac{\lambda f(t)}{\lambda_C} \right] \xi + a \xi^2 = \left[ \frac{\lambda f(t)}{\lambda_C} \right] \bar{\xi} \quad (28)$$

when terms in  $\xi$  of degree higher than quadratic are dropped. Here

$$\omega_1^2 = \frac{M(\underline{u}_1) \cdot \underline{u}_1}{\underline{g}_1 \cdot \underline{e}_1}$$

and so it is recognized that if  $\underline{u}_1$  happens to be a natural vibration mode,  $\omega_1$  is its natural frequency; otherwise,  $\omega_1^2$  has an interpretation as a Rayleigh quotient for frequency-squared, based on the buckling mode  $\underline{u}_1$ . It will be convenient to refer to  $\omega_1$  as the "frequency" of the mode  $\underline{u}_1$ , whether or not this buckling mode is truly a natural vibration mode.

In the case of the cubic structure, assuming

$$\underline{u} = \lambda f(t)\underline{u}_0 + \xi(t)\underline{u}_1 + \xi^2(t)\underline{u}_2 \quad (29)$$

and dropping terms containing  $M(\underline{u}_2)$  or  $M(\underline{u}_0)$  gives the equation

$$\left(\frac{1}{\omega_1^2}\right)\ddot{\xi} + \left[1 - \frac{\lambda f(t)}{\lambda_C}\right]\xi + b\xi^3 = \left[\frac{\lambda f(t)}{\lambda_C}\right]\bar{\xi} \quad (30)$$

as the result of a Galerkin solution of (29), with  $\delta\underline{u} = \underline{u}_1\delta\xi$ .\*

Equations (28) and (30) have the simple mechanical interpretation shown in Figure 2, wherein  $\xi$  is the additional displacement of the central hinge of the two-bar simply-supported column subjected to an axial load  $\lambda f(t)$ . The bars of unit length are rigid but weightless, the central hinge carries a mass  $M$ , and the force-displacement relation of the non-linear spring at the central hinge is either  $F = K(\xi+a\xi^2)$  or  $F = K(\xi+b\xi^3)$ . Then, with  $\omega_1^2 = K/M$  and  $\lambda_C = \frac{K}{2}$ , and an initial displacement  $\bar{\xi}$ , Equations (28) and (30) govern the

\* Note that the neglect of  $M(\underline{u}_0)$  is consistent with taking the coefficient of  $\underline{u}_0$  as simply  $\lambda f(t)$  in (27) and (29); significant inertial effects associated with  $\underline{u}_0$  would invalidate this assumption of a "static" response in the "trivial" mode. Similarly, neglecting the inertia of the "contaminating" mode  $\underline{u}_2$  is consistent with retaining the old static relation between  $\underline{u}_2$  and  $\underline{u}_1$  in (29). Quite apart from such considerations, it may be noted that the terms  $M(\underline{u}_0)\cdot\underline{u}_1$  and  $M(\underline{u}_2)\cdot\underline{u}_1$  which appear in the Galerkin solution of (26) when  $\delta\underline{u}$  is taken as  $\underline{u}_1\delta\xi$  can be shown to vanish if  $\underline{u}_1$  happens to be a natural vibration mode; under this circumstance the variational equation of equilibrium for vibration modes gives  $\omega_1^2 M(\underline{u}_1)\cdot\delta\underline{u} = \sigma_1\cdot\delta\underline{e}$ , but since, by (15),  $\sigma_1\cdot\underline{u}_2 = \sigma_1\cdot\underline{u}_0 = 0$ , it follows that  $M(\underline{u}_1)\cdot\underline{u}_2 = M(\underline{u}_1)\cdot\underline{u}_0 = 0$ , whence  $M(\underline{u}_2)\cdot\underline{u}_1 = M(\underline{u}_2)\cdot\underline{u}_1 = 0$  by the reciprocity properties of the operator  $M$ .

additional displacement  $\xi$  in the case of quadratic and cubic springs, respectively.\*

Step loading

The imperfection-sensitive cubic structure governed by Equation (30), with  $b < 0$ , will be studied for the case of step loading, for which  $f(t) \equiv H(t)$ , the Heaviside step function, which vanishes for  $t \leq 0$  and equals unity for  $t > 0$ . A first integral of Equation (30) is readily found to be

$$\frac{(\dot{\xi})^2}{2\omega_1^2} + \left(1 - \frac{\lambda}{\lambda_C}\right) \frac{\xi^2}{2} + \frac{b\xi^4}{4} = \left(\frac{\lambda}{\lambda_C}\right) \bar{\xi} \xi \quad (31)$$

from which it follows that the maximum displacement  $\xi_{\max}$  -- if a maximum exists -- must satisfy

$$\left(1 - \frac{\lambda}{\lambda_C}\right) \frac{\xi_{\max}^2}{2} + \frac{b\xi_{\max}^4}{4} = \left(\frac{\lambda}{\lambda_C}\right) \bar{\xi} \xi_{\max} \quad (32)$$

or (see Figure 3)

$$\frac{\lambda}{\lambda_C} = \frac{2\xi_{\max} + b\xi_{\max}^2}{2\xi_{\max} + 4\bar{\xi}} \quad (33)$$

For sufficiently low positive values of  $\lambda/\lambda_C$ ,  $\xi(t)$  is bounded and periodic, (as a phase-plane study of (31) quickly reveals), and  $\xi_{\max}$  is given by the lower solution of Equation (32), as shown by the solid part of the curve in Figure 3. But, as Figure 3 illustrates, for  $b < 0$ , there is a maximum value of  $\lambda$  for which a bounded  $\xi(t)$  exists, and it is this maximum value that will be defined as the dynamic buckling load  $\lambda_D$ . This critical value  $\lambda_D$  satisfies  $d\lambda/d\xi_{\max} = 0$ , and for values of  $\lambda$  greater than  $\lambda_D$  the response

---

\* In this model, non-linear geometrical effects introduce additional terms of order  $\xi^3$  which are being ignored relative to those in the non-linear spring characteristic.

$\xi(t)$  is monotonic and unbounded. It is readily found that  $\lambda_D$  must satisfy

$$\left(1 - \frac{\lambda_D}{\lambda_C}\right)^{\frac{3}{2}} = \frac{3\sqrt{6} \sqrt{-b} |\bar{\xi}|}{2} \left(\frac{\lambda_D}{\lambda_C}\right) \quad (34)$$

The next step sets a pattern to be followed repeatedly in the present studies; the term  $\sqrt{-b} |\bar{\xi}|$  is eliminated between Equation (34) for dynamic buckling and Equation (25) for static buckling of the same structure with the same imperfection. This gives as the final result for the analysis of dynamic buckling of a cubic structure under step loading the relation

$$\frac{\left[1 - \left(\frac{\lambda_D}{\lambda_S}\right)\left(\frac{\lambda_S}{\lambda_C}\right)\right]^{\frac{3}{2}}}{1 - \left(\frac{\lambda_S}{\lambda_C}\right)} = \sqrt{2} \left(\frac{\lambda_D}{\lambda_S}\right) \quad (35)$$

This relation between  $(\lambda_D/\lambda_S)$  and  $(\lambda_S/\lambda_C)$  is shown by the dotted curve in Figure 4. An entirely similar analysis for a quadratic structure, with  $(a\bar{\xi}) < 0$ , gives the analogous result

$$\frac{\left[1 - \left(\frac{\lambda_D}{\lambda_S}\right)\left(\frac{\lambda_S}{\lambda_C}\right)\right]^2}{1 - \left(\frac{\lambda_S}{\lambda_C}\right)} = \frac{4}{3} \left(\frac{\lambda_D}{\lambda_S}\right) \quad (35)$$

represented by the solid curve in Figure 4.

The results (35) and (36) are to be viewed as providing estimates for the ratio  $(\lambda_D/\lambda_S)$  in an imperfection-sensitive structure in terms of the known -- or assumed -- values of  $(\lambda_S/\lambda_C)$  of the same structure. The more imperfect the structure -- and the greater its imperfection-sensitivity -- the lower will be  $\lambda_S/\lambda_C$ , and hence the lower will be the ratio  $\lambda_D/\lambda_S$  of dynamic to static buckling strength. Note, however, that  $\lambda_D/\lambda_S$  will never be less than  $\sqrt{2}/2$ . Note, too, that the use of these results for  $\lambda_D/\lambda_S$  are consistent with the

design of structures on a statistical basis; if under the static loading  $\lambda_S$  a structure enjoys a certain probability of withstanding static buckling, it will resist dynamic buckling with the same reliability under the dynamic load  $(\lambda_D/\lambda_S)(\lambda_S)$  when the dependence of  $(\lambda_D/\lambda_S)$  on  $(\lambda_S/\lambda_C)$  is that given by Figure 4.

Impulsive loading

Now consider the impulsive loading specified by the relation

$$\lambda f(t) = I\delta(t) \quad (37)$$

where  $\delta$  is the Dirac delta function. Considering first the cubic structure, it is easily found that

$$(\dot{\xi})_{0+} = \frac{\omega_1^2 I \bar{\xi}}{\lambda_C}$$

and so a first integral of (30) is

$$\frac{(\dot{\xi})^2}{2\omega_1^2} + \frac{\xi^2}{2} + \frac{b\xi^4}{4} = \frac{1}{2} \left( \frac{I\bar{\xi}}{\lambda_C} \right)^2 (\omega_1^2)$$

A bounded value of  $(\xi)_{\max}$  is now found to exist only for  $I < I_{cr}$ , where

$$I_{cr} = \frac{\frac{1}{\sqrt{2}} \left( \frac{\lambda_C}{\omega_1} \right)}{|\bar{\xi}| \sqrt{-b}} \quad (38)$$

and therefore  $I_{cr}$  is defined as the dynamic buckling impulse. Eliminating  $|\xi| \sqrt{-b}$  between (38) and (25) now gives

$$I_{cr} = \frac{\frac{3\sqrt{6}}{4} \left( \frac{\lambda_S}{\omega_1} \right)}{\left( 1 - \lambda_S/\lambda_C \right)^{3/2}} \quad (39)$$

as the relation between  $I_{cr}$ ,  $\lambda_S$ ,  $\lambda_C$ , and  $\omega_1$ . A limiting result for a very imperfect structure, for which one can let  $\lambda_S/\lambda_C = 0$ , is simply

$$I_{cr} = \frac{3\sqrt{6}}{4} \left( \frac{\lambda_S}{\omega_1} \right) \approx 1.84 \left( \frac{\lambda_S}{\omega_1} \right) \quad (40)$$

and this could be used as a conservative estimate for  $I_{cr}$  for other values of  $\lambda_S/\lambda_C$ .

Repetition of the analysis for the case of the quadratic structure described by (28) gives

$$I_{cr} = \frac{\frac{4\sqrt{3}}{3} \left( \frac{\lambda_S}{\omega_1} \right)}{1 - \left( \frac{\lambda_S}{\lambda_C} \right)^2} \quad (41)$$

with

$$I_{cr} \approx 2.31 \left( \frac{\lambda_S}{\omega_1} \right) \quad (42)$$

as the critical impulse for the very imperfect structure. Note that, as in the case of step loading, more conservative answers are given by the cubic structure.

### Transient loading

Consider next the rectangular loading history

$$\begin{aligned} f(t) &= 1 && \text{for } t < T \\ f(t) &= 0 && \text{for } t < 0, t > T \end{aligned}$$

As shown in an earlier paper (Hutchinson and Budiansky, 1966)  $\lambda_D$  can, again, be defined as the highest value of  $\lambda$  for which a bounded response exists, when either (28) or (30) is used to characterize the structure. Fairly straightforward calculation procedures were used to find  $\lambda_D$ , and typical of the results obtained are the curves shown in Figure 5, for the cubic structure. Each curve corresponds to a different value of  $T/T_1$ , the ratio of the loading duration to the period of vibration  $T = \frac{2\pi}{\omega_1}$  of the buckling mode. Note that the case  $T/T_1 = \infty$  is the same as the step-loading situation previously considered.

The most significant implication of Figure 5 is that loads much in excess of the static buckling load can be applied to imperfection-sensitive structures without the occurrence of dynamic buckling, if they are removed soon enough; further, for a given duration of loading, the extent to which the static buckling load may be exceeded rises very sharply with increasing perfection of the structure (that is, with increasing  $\lambda_S/\lambda_C$ ).

Informative cross-plots of the data in Figure 5 are shown in Figure 6, wherein the finite-time-impulse parameter  $I_T = \lambda_D T$  has been introduced. In Figure 6,  $I_T/I_{cr}$ , where  $I_{cr}$ , as given by (39), is the zero-time critical impulse, is plotted against the load-duration parameter  $T/T_1$  for various values of  $\lambda_S/\lambda_C$ . The very important fact shown here is that, contrary to what might be expected, the zero-time critical impulse is not generally a good approximation to the finite-time impulse  $I_T$  needed to produce dynamic buckling. Indeed, even if  $T/T_1$  is very low,  $I_{cr}$  constitutes an unconservative approximation to  $I_T$ , except when the structure is quite imperfect ( $\lambda_S/\lambda_C \approx 1/10$ ).

Additional results have been given for quadratic structures (Hutchinson and Budiansky, 1966), and for structures under suddenly applied loads that decay linearly with time.

#### Discussion

The results obtained on the basis of the simple equations (28) and (30) should clearly be regarded only as generalized estimates that could be subject to severe limitations on their validity. Perhaps the most serious simplifying assumption made was that the dynamic response could be described adequately in terms of the deformation pattern that occurs when the structure buckles statically. This does not seem too unreasonable in the case of a structure



having well-separated eigenvalues as the solutions to the classical static buckling problem, the lowest of which is associated with a single eigenfunction; but when these conditions are not met, as in the cases of multiple classical buckling modes, or when continuous (or nearly continuous) spectra of eigenvalues exist in the vicinity of the lowest classical buckling mode, the results found may justifiably be viewed with suspicion.

Other questionable simplifications, perhaps less important, are the neglect of prebuckling inertia and the disregard of degrees of non-linearity higher than the lowest. All of these effects will be explored to some extent in the rest of this paper. But first consideration will be given to generalized criteria for dynamic buckling, since the simple criterion related to the existence of bounded solutions that has been used until now becomes inadequate when idealizations more complicated than those embodied in the simple equations (28) and (30) are introduced.

#### GENERALIZED CRITERIA FOR DYNAMIC BUCKLING

##### Single-mode analyses

If the quadratic model described by (28), with  $a < 0$ ,  $\bar{\xi} > 0$ , is turned into a quadratic-cubic model by the incorporation of a stabilizing cubic term  $b\xi^3$ , with  $b > 0$ , so that

$$\left(\frac{1}{\omega_1^2}\right)\ddot{\xi} + \left(1 - \frac{\lambda f}{\lambda_C}\right)\dot{\xi} + a\xi^2 + b\xi^3 = \left(\frac{\lambda f}{\lambda_C}\right)\bar{\xi} \quad (43)$$

a bounded response  $\xi(t)$  occurs for all  $\lambda$ , but sharp definitions of dynamic buckling are still often possible. In the case, for example, of step loading, it is easily shown that, for sufficiently small  $\bar{\xi}$ ,  $\xi_{\max}$  varies with  $\lambda$  as shown in Figure 7(a), when, as before, ensembles of loading histories  $\lambda H(t)$

and the associated responses  $\xi(t)$  are contemplated. At a critical value of  $\lambda$ , to be defined as  $\lambda_D$ , a finite jump in  $\xi_{\max}$  is produced by an infinitesimal increase in  $\lambda$ . From (43), the relation between  $\lambda$  and  $\xi_{\max}$  is found to be simply

$$\left(1 - \frac{\lambda}{\lambda_C}\right)\xi_{\max} + \frac{2a\xi_{\max}^2}{3} + \frac{1}{2}b\xi_{\max}^3 = 2\left(\frac{\lambda}{\lambda_C}\right)\bar{\xi} \quad (44)$$

but that part of the curve given by (44) that is shown dotted in Figure 7(a) is without physical significance. (For all  $\lambda \neq \lambda_D$ , the response  $\xi(t)$  is periodic; as  $\lambda$  approaches  $\lambda_D$  from below the period approaches infinity, and it takes an infinitely long time for  $\xi(t)$  to reach  $\xi_{\max}$ . For  $\lambda$  larger than  $\lambda_D$ , the period drops to a finite value again.) The value of  $\lambda_D$  occurs at the first maximum of the relation (44) for  $\lambda$  vs.  $\xi_{\max}$ , just as  $\lambda_S$  is the first maximum of the static relation between  $\lambda$  and  $\xi$  given by (43) (with the dynamic term deleted) shown schematically in Figure 7(c).

For  $\bar{\xi}$  sufficiently large, the variation of  $\lambda$  with  $\xi_{\max}$  given by (44) becomes monotonic, as sketched in Figure 7(b), and the sharp definition of  $\lambda_D$  afforded by the relation of Figure 7(a) is lost even though for the same value of  $\bar{\xi}$  it may still be possible for there to be static snap buckling of the kind implied by Figure 7(c). It may be desirable, then, to retain the concept of dynamic buckling by letting  $\lambda_D$  be associated with the point of inflection in the variation of  $\lambda$  with  $\xi_{\max}$ . This appears to be a reasonably practical criterion for  $\lambda_D$ , so long as the inflection in the curve is pronounced enough to imply that small changes in  $\lambda$  near  $\lambda = \lambda_D$  actually do lead to large changes in the response.

Apart from the question of defining  $\lambda_D$  for the system described by (43),

it may be of interest to examine how much the results found deviate from those already obtained for  $b = 0$ . Calculations\* for the case of step loading give the curves in Figure 8 for  $\frac{b}{a^2} = \frac{1}{3}$  and  $\frac{2}{3}$ . The solid parts of the curves apply when dynamic buckling is associated with the "jump" condition of Figure 7(a); the dotted portions correspond to the point-of-inflection criterion of Figure 7(b). (The curve for  $b/a^2 = \frac{2}{3}$  stops at  $\lambda_S/\lambda_C = \frac{1}{2}$  because static snap-buckling of the kind that corresponds to Figure 7(c) does not occur for lower values of  $\lambda_S/\lambda_C$ , since even the static curve of  $\lambda$  vs.  $\xi$  becomes monotonic for imperfections higher than that associated with the end-point of the curve.) Comparison with the curve for  $b = 0$ , reproduced from Figure 4, shows that a stabilizing term  $b\xi^3$  just makes the old results slightly conservative. Similar calculations for impulsive loading give the curves of Figure 9, wherein the ratio of critical impulse to that of the case with  $b = 0$  is given as a function of  $\lambda_S/\lambda_C$  for several values of  $b/a^2$ . Again, the dotted curves follow from a point-of-inflection criterion. As the auxiliary sketches show, for  $b/a^2$  larger than about 1/3 the variation of  $I$  with  $\xi_{\max}$  no longer displays a very sharp break near the inflection point. Thus, where  $I_{cr}$  retains meaningful significance as a buckling impulse, the simple model still gives conservative results.

More or less similar trends have been discovered from calculations based on the differential equation for a cubic-quartic model

$$\left(\frac{1}{\omega_1^2}\right)\ddot{\xi} + \left(1 - \frac{\lambda f}{\lambda_C}\right)\dot{\xi} + b\xi^3 + c\xi^4 = \left(\frac{\lambda f}{\lambda_C}\right)\bar{\xi} \quad (45)$$

---

\* The author is indebted to Mr. John Wivorkoski for calculating these results.

wherein a stabilizing term  $c\xi^4$  ( $c > 0$ ) is added to the cubic-model equation (30). Again, the old results of Figure 4 and Equation (39) are conservative when the modified definitions of  $\lambda_D$  or  $I_{cr}$  are used, and where the point-of-inflection criterion really constitutes a sharp measure of buckling.

Multi-mode analyses

Suppose next that the behavior of the dynamical structural system being studied can no longer be adequately described on the basis of a single-mode representation, but rather requires the solution of a set of ordinary, nonlinear differential equations of the form, say,

$$\left(\frac{1}{\omega_n^2}\right)\ddot{\xi}_n + Q_n[\xi_1, \xi_2, \dots, \xi_n; \lambda f(t)] = 0 \quad (46)$$

(n=1,2,...N)

Dynamic buckling criteria for the establishment of  $\lambda_D$  of the types suggested by Figures 7(a) and 7(b) could still be used if one of the  $\xi$ 's is used as abscissa, or, perhaps more appropriately, if the abscissa is replaced by some overall measure of the response (as, for example,  $|\vec{\xi}| \equiv \sqrt{\sum_1^N \xi_n^2}$ ). In either case some interesting questions arise. Is it possible to know whether the sharp jump criterion of Figure 7(a) will apply in the multi-mode case? If so, might it be possible to estimate  $\lambda_D$  without the necessity of actually solving the differential equations (46) in detail for many values of  $\lambda$ ? Such questions have recently been discussed by Humphreys (1966) and the remarks that follow lean heavily on his observations.

An illustrative two-degree-of-freedom problem can be associated with the diagram of Figure 10(a) showing contour lines of constant elevation on a perfectly smooth terrain. Imagine a particle of unit mass initially at the bottom of one of the two bowls ( $\xi_1 = \xi_2 = 0$ ) and suppose it to be subjected to an impulse  $I$  in the  $\xi_1$  direction. It seems evident that there must

exist a critical impulse just sufficient to send the particle over the pass into the next bowl, so that a plot of impulse versus the maximum excursion  $|\xi|$  will exhibit a jump. The kinetic energy imparted to the particle of unit mass by the critical impulse can clearly not be less than the elevation at the saddle point (3 units) and, indeed, the analogue of this lower bound was actually used by Hoff and Bruce (1954) to estimate dynamic buckling loads in an arch buckling problem. But there is no evident reason to expect that an initial kinetic energy equal to the saddle point energy is sufficient as well as necessary for "buckling" and, unfortunately, it is not clear that the correct value of  $I_{cr}$  can be found without actually solving for  $\xi_1(t)$  and  $\xi_2(t)$  for many values of  $I$ . Finally, it must be realized that the terrain might look like that shown in Figure 10(b). The profiles of the surfaces of Figures 10(a) and (b) are identical along  $\xi_2 = 0$ , and suppression of the  $\xi_2$  degree of freedom would be consistent with a jump in the curve of  $I$  versus  $\xi_1$  which would then be applicable to both problems. But in the bowl-with-ridge case of Figure 10(b) a jump can no longer occur when the two-degree-of-freedom situation is analyzed, although it may still be possible to define a "practical"  $I_{cr}$  associated with a point-of-inflection criterion.

It may be remarked that if the functions  $Q_n$  in (46) are continuous then over any finite time interval  $(0,T)$  the solutions must be continuous functions of  $\lambda$ ; the jump criterion for dynamic buckling, if applicable at all, can only work in principle if the response measure is maximized over an infinite time interval. Hence, if multi-mode problems are to be studied numerically for the determination of  $\lambda_D$ , and solutions are therefore found for finite time durations, only the point-of-inflection criterion can really be used.

(Numerical calculation has shown, however, that the breaks in the curves of  $\lambda$

versus maximum response in  $(0, T)$  are often so sharp that they look like discontinuous jumps.)

SOME MULTI-MODE STUDIES

Inertia of the prebuckling mode; Mathieu coupling

The assumption made concerning the neglect of the inertial forces associated with the prebuckling deformation mode  $\underline{u}_0$  precludes the possibility of discussing the kind of instability studied by Goodier and McIvor (1964) wherein oscillations in the prebuckling deformation mode feed energy into a buckling mode. An attempt will now be made to estimate the conditions under which this phenomenon might be expected to intrude upon the results that have been obtained in the present paper for dynamic buckling loads.

Consider the quadratic structure, and replace the Galerkin assumption (27) by the expression

$$\underline{u} = \xi_0 \underline{u}_0 + \xi_1 \underline{u}_1 \tag{47}$$

in the dynamic equilibrium equation (26). Assuming, for simplicity, that  $\underline{u}_1$  is a natural vibration mode, the variation  $\delta \underline{u} \equiv \underline{u}_0$  in (26) then gives

$$\left( \frac{1}{\omega_0^2} \right) \ddot{\xi}_0 + \xi_0 = \lambda f \tag{48}$$

wherein terms of order  $\xi^2$  and  $\xi \bar{\xi}$  have been dropped, and where  $\omega_0 = \left[ \frac{M(\underline{u}_0) \cdot \underline{u}_0}{\sigma_0 \cdot \xi_0} \right]^{1/2}$  is the "frequency" of the prebuckling mode. Taking  $\delta \underline{u} \equiv \underline{u}_1$  gives

$$\left( \frac{1}{\omega_1^2} \right) \ddot{\xi}_1 + \left( 1 - \frac{\xi_0}{\lambda_C} \right) \xi_1 + a \xi_1^2 = \left( \frac{\xi_0}{\lambda_C} \right) \bar{\xi} \tag{49}$$

to order  $\xi^2$ . Now consider step loading, for which the solution of (48) is

$$\xi_0 = \lambda(1 - \cos \omega_0 \tau) \tag{50}$$

Substitution of (50) into (49) gives the relation

$$\frac{d^2 \xi_1}{d\tau^2} + \left[ \left( 1 - \frac{\lambda}{\lambda_C} \right) \left( \frac{\omega_1}{\omega_0} \right)^2 + \left( \frac{\lambda}{\lambda_C} \right) \left( \frac{\omega_1}{\omega_0} \right)^2 \cos \tau \right] \xi_1 + (\text{non-linear terms}) = \frac{\lambda(1-\cos \tau) \bar{\xi}}{\lambda_C} \quad (51)$$

where  $\tau = \omega_0 t$ . Now the linear terms in  $\xi$  are precisely those that appear in the Mathieu equation, and, in the absence of all of the nonlinear terms in (51), would lead to instability of the Mathieu type for certain combinations of  $\lambda/\lambda_C$  and  $(\omega_1/\omega_0)$ . From the known properties of solutions to Mathieu's equation (see, for example, Stoker, 1950), the following question can now be answered: For what combinations of  $\lambda_S/\lambda_C$  and  $\left(\frac{\omega_1}{\omega_0}\right)$  will the linearized equation (51) have stable solutions when  $\lambda = \lambda_D$ , as given by Figure 4? Such combinations of  $\lambda_S/\lambda_C$  and  $\omega_1/\omega_0$  (for  $\frac{\omega_1}{\omega_0} < 1$ ) are given by the doubly-hatched region of Figure 11. In the singly-hatched region, while there is no Mathieu instability at  $\lambda = \lambda_D$ , there nevertheless are instabilities at lower values of  $\lambda$ . This chart completely neglects, of course, interaction between the two phenomena whose potential interaction is being assessed and must, therefore, be regarded as no more than suggestive. It is nevertheless difficult to believe, that for values of  $\omega_1/\omega_0$  less than, say,  $1/4$ , there would be any need for concern about a Mathieu-type instability before the occurrence of dynamic buckling under step loading. The situation turns out to be not quite so optimistic for impulsive loading. Impulsive loading  $\lambda f(t) = I\delta(t)$  gives

$$\xi_0 = I\omega_0 \sin \omega_0 t$$

as the solution of (48), and then the linear, homogeneous part of (49) gives the Mathieu equation

$$\frac{d^2 \xi_1}{d\tau^2} + \left[ \left( \frac{\omega_1}{\omega_0} \right)^2 - \left( \frac{I\omega_1}{\lambda_C} \right) \left( \frac{\omega_1}{\omega_0} \right) \sin \tau \right] \xi_1 = 0$$

Once again, the known behavior of solutions to Mathieu's equation and the results found earlier for  $I_{cr}$  provides the information in Figure 12(a), the cross-hatched regions of which show combinations of  $\lambda_S/\lambda_C$  and  $\left( \frac{\omega_1}{\omega_0} \right)$  for which Mathieu instability is induced at  $I = I_{cr}$  as given by (41), or at some lower  $I$ . On the other hand, if the conservative estimate  $I_{cr} = 2.31 \left( \frac{\lambda_S}{\omega_1} \right)$  is used, those regions shrink to the domain shown in Figure 12(b).

All of these concerns about the possibility of Mathieu-type resonances should be tempered somewhat by the realization that Mathieu instability is often associated with many cycles of an oscillation that grows in amplitude as opposed to the "one-shot" dynamic buckling contemplated by the criteria of this paper. Thus, damping may be expected to be more effective in alleviating the potential dangers of a Mathieu instability than it would in retarding a more-or-less monotonic dynamic buckling.

#### Axially compressed cylinders

The static post-buckling analysis of a long axially compressed circular cylinder differs from the general patterns already given because there exist many different modes at one and the same buckling stress. But, following Koiter, the analysis can be extended to handle such cases, and in the case of the cylinder an approach that seems to provide insight into the post-buckling behavior has been followed (Budiansky and Hutchinson, 1964) by letting the initial and additional normal displacements be

$$\bar{w} = \bar{\xi}_1 w(1) + \bar{\xi}_2 w(2)$$

$$w = \xi_1 w(1) + \xi_2 w(2)$$



respectively, where  $w^{(1)}$  is the axisymmetric buckling mode and  $w^{(2)}$  is the square-buckle mode. Using (51) in a Galerkin solution of (26) (in conjunction with Donnell's equation) then leads to the two coupled equations

$$\begin{cases} \left(\frac{1}{\omega_1}\right)^2 \ddot{\xi}_1 + \left(1 - \frac{\lambda f}{\lambda_C}\right) \xi_1 - e \xi_2^2 = \left(\frac{\lambda f}{\lambda_C}\right) \bar{\xi}_1 \\ \left(\frac{1}{\omega_2}\right)^2 \ddot{\xi}_2 + \left(1 - \frac{f}{C}\right) \xi_2 - 16e \xi_1 \xi_2 = \left(\frac{\lambda f}{\lambda_C}\right) \bar{\xi}_2 \end{cases} \quad (52)$$

where, it turns out,  $\omega_2 = \frac{1}{2} \omega_1$ , and  $e = \frac{3\sqrt{3(1-\nu)}}{32}$ . Dropping the time dependent terms, (and taking  $f \equiv 1$ ), permitted the evaluation of  $\lambda_S$  for a variety of values of  $\bar{\xi}_1$  and  $\bar{\xi}_2$ . Then  $\lambda_D$  was found, for step-loading, for the same values of  $\bar{\xi}_1$  and  $\bar{\xi}_2$ , by solving the differential equation numerically and using as the criterion for dynamic buckling the sharp transition from bounded to unbounded response that was very evident from the numerical results. It was found that the lower curve of Figure 4 always gave conservative estimates for  $\lambda_D/\lambda_S$ . The lowest values of  $\lambda_D/\lambda_S$  occurred for  $\bar{\xi}_1 = 0$ . For this case, an excellent analytical approximation is found by neglecting the inertia of the axisymmetric mode, in which case one finds

$$\left(\frac{1 - \lambda_D/\lambda_C}{1 - \lambda_S/\lambda_C}\right)^2 = \sqrt{2} (\lambda_D/\lambda_S) \quad (53)$$

and this equation gives a relation between  $\lambda_D/\lambda_S$  and  $\lambda_C/\lambda_S$  which lies between the two curves in Figure 4.

Similarly detailed studies have not been made for impulsive loading but it is interesting that making the same assumptions  $\bar{\xi}_1 = 0$  and  $\omega_1 = \infty$  that were so useful in the step-loading case leads to

$$I_{cr} = \frac{\frac{3\sqrt{6}}{4} \left(\frac{\lambda_S}{\omega_2}\right)}{\left[1 - \frac{\lambda_S}{\lambda_C}\right]^2} \quad (54)$$

which is between the results (39) and (41) for the quadratic and cubic models. (Here  $\omega_2$  is  $\frac{\sqrt{2}}{2R} \sqrt{\frac{E}{\rho}}$ , where  $R$  = cylinder radius,  $E$  = Young's modulus, and  $\rho$  = density.)

These results for the cylinder, though they have a certain internal plausibility, can not, of course, be regarded as more than suggestive of the range in which critical loads and impulses might lie. The reason is that not only have just two of the many existing classical modes been considered but also the multitude of modes associated with eigenvalues higher, but close to, the lowest critical stress has been ignored. Imperfections in all of these modes, and the different natural frequencies of the modes, may be expected to enter into the dynamic buckling process in a way that formulas like (53) and (54) can simply not encompass. To provide insight into such questions, some results of a many-mode study of an artificial structure having random imperfections is given next. As will be seen, the results will suggest that (54) for impulsive loading is probably less reliable than (53) for step loading.

#### A SPECIAL MANY-MODE STUDY

The problem to be discussed is that of the static and dynamic buckling of an infinitely long column (see Figure 13) having a random initial lateral displacement, and supported laterally by a continuous elastic foundation that provides the non-linear (cubic) restoring force per unit length

$$q = k_1 w - k_3 w^3 \quad (k_1, k_3 > 0) \quad (55)$$

where  $w$  is the additional displacement induced by an axial load  $\lambda f(t)$ . This structure may clearly be expected to be imperfection-sensitive, because of the "softening" spring support. Ignoring (as in the case of the cubic model of Figure 2) non-linear geometrical effects, and also neglecting wave effects

due to axial inertia, permits the derivation of the differential equation of motion

$$m \frac{\partial^2 w}{\partial t^2} + EI \frac{\partial^4 w}{\partial x^4} + \lambda f \frac{\partial^2 w}{\partial x^2} + k_1 w - k_3 w^3 = -\lambda f \frac{\partial^2 \bar{w}}{\partial x^2} \quad (56)$$

where  $EI$  is the bending stiffness,  $m$  is mass per unit length, and  $\bar{w}$  is the initial displacement. The perfect structure has the static buckling modes  $w = \sin \frac{v x}{\left(\frac{EI}{k_1}\right)^{1/4}}$  corresponding to buckling loads  $\lambda = (EI k_1)^{1/2} \left(v + \frac{1}{v}\right)$ , so that the critical (lowest) buckling load is  $\lambda_1 = \lambda_C = 2\sqrt{EI k_1}$ , corresponding to  $v = 1$ . The buckling modes are also vibration modes of the unloaded perfect structure, corresponding to frequencies

$$\omega = \left(\frac{k_1}{m}\right)^{1/2} (1+v^4)^{1/2}$$

and the frequency of the critical buckling mode is then

$$\omega_1 = \sqrt{2} \left(\frac{k_1}{m}\right)^{1/2} \quad (57)$$

The contrast between this structure and the simple model of Figure 2 can now be underscored. Instead of a single buckling mode associated with a single buckling load, there is a continuous spectrum of buckling loads and modes; similarly, there is a continuous spectrum of vibration frequencies. Uncritical application of the dynamic buckling results for the simple model would involve only  $\lambda_1$ , the lowest buckling load, and  $\omega_1$ , the frequency of this mode. But clearly, one should expect deviations from the elementary results, and the purpose of this study is to explore these deviations.

The differential equation (56) can now be conveniently non-dimensionalized by letting  $\bar{\Delta}$  be the root-mean-square value of the initial imperfection  $\bar{w}$ , and introducing

$$u = \frac{w}{\Delta} \quad y = \frac{x}{\left(\frac{EI}{k_1}\right)^{1/4}}$$

$$\bar{u} = \frac{\bar{w}}{\Delta} \quad \tau = \left(\frac{\omega_1}{\sqrt{2}}\right)\tau$$

to get

$$\ddot{u} + u^{IV} + 2\left(\frac{\lambda f}{\lambda C}\right)u'' + u - ru^3 = -2\left(\frac{\lambda f}{\lambda C}\right)\bar{u}'' \quad (58)$$

where  $(\dot{\phantom{x}}) = \frac{\partial}{\partial \tau}$ ,  $(\phantom{x})' = \frac{\partial}{\partial y}$ , and  $r = \frac{k_3 \Delta^2}{k_1}$ .

The problem of finding the static buckling load  $\lambda_S$  for imperfections described by a stationary random Gaussian function  $\bar{u}$  has been solved approximately (Fraser, 1965) by the method of equivalent linearization. In this

work the correlation function for  $\bar{u}$ , defined by  $R(\zeta) = \lim_{l \rightarrow \infty} \frac{1}{l} \int_{-l}^l \bar{u}(y)\bar{u}(y+\zeta)dy$  was chosen as

$$R(\zeta) = e^{-k|\zeta|} \cos c\zeta \quad (59)$$

giving the corresponding power spectral density

$$S(\phi) = \frac{1}{2\pi} \int_{-\infty}^{\infty} R(\zeta) e^{-i\phi\zeta} d\zeta = \frac{k(\phi^2 + k^2 + c^2)}{\pi[\phi^4 + 2(k^2 - c^2)\phi^2 + (k^2 + c^2)^2]} \quad (60)$$

The method of equivalent linearization involved the replacement of  $ru^3$  in Equation (58) by  $\epsilon u$ , the subsequent deduction from the static form of (58), of  $\Delta^2 \equiv (u^2)_{ave}$  as a function of  $k$ ,  $c$ ,  $\frac{\lambda}{\lambda_C}$ , and  $\epsilon$ , and finally the use of the assumption

$$(u^4)_{ave} = 3(u^2)_{ave} \quad (61)$$

appropriate to a linear Gaussian process to deduce the condition

$$\varepsilon = 3r \Delta^2$$

from the stipulation  $\varepsilon(u^2)_{\text{ave}} = r(u^4)_{\text{ave}}$ . With the elimination of  $\varepsilon$  the implicit relation thus developed between  $\lambda/\lambda_C$  and  $\Delta^2$  (for given values of  $k$ ,  $c$ , and  $r$ ) then permitted the discovery of a maximum value of  $\lambda$ , identified as  $\lambda_S$ .

A similar procedure can be followed in conjunction with the full dynamic equation (58). For the case of step loading, replacing  $ru^3$  by  $\rho u$  leads to the interesting conclusion that as  $\tau$  becomes infinite,  $\Delta^2$  approaches a definite limit that depends only on  $\lambda/\lambda_C$ ,  $k$ ,  $c$ , and  $\rho$ . In the dynamic case, the assignment of a value for  $\rho$  stems from a consideration of an averaging process involving a first time integral of (58), and gives

$\rho(u^2)_{\text{ave}} = \frac{r}{2} (u^4)_{\text{ave}}$ , so that, when (61) is invoked,  $\rho = \frac{3}{2} r \Delta^2$ . Elimination of  $\rho$  then provides a relation between  $\lambda/\lambda_C$  and the limiting value of  $\Delta^2$  as  $\tau \rightarrow \infty$ . The condition for calculating the dynamic buckling load  $\lambda_D$  is, finally, taken as the non-existence of this limit. An entirely similar procedure works for impulsive loading and the calculation of  $I_{cr}$ .

The details of the calculations described will be presented elsewhere, but a few interesting numerical results will now be discussed. It was found that for a very wide range of values of  $k$  and  $c$  in the assumed correlation function for the imperfections, the variation of  $\lambda_D/\lambda_S$  with  $\lambda_S/\lambda_C$  for the case of step loading remained in the very narrow band shown in Figure 14. Furthermore, quite independently of  $k$  and  $c$ , the limiting value of  $\lambda_D/\lambda_S$  for the case of a very imperfect structure ( $\lambda_S/\lambda_C \rightarrow 0$ ) is  $2/\sqrt{3} \approx 1.15$ .

These results -- dynamic buckling loads higher than static for step loadings -- seem paradoxical but their derivation is vulnerable only in the use of the method of equivalent linearization. With a little effort, it is

possible to accept their plausibility as a consequence of phase interference among many modes that happens to be more effective dynamically than statically.\* In any case, the results surely tend to reinforce one's confidence in the reliability of the predictions for dynamic buckling under step loading based on the simple one-degree-of-freedom models.

The calculations made for impulsive loading do not allow such optimistic conclusions. Just some results for the limiting case of a very imperfect structure will be displayed by showing in Figure 15 how the ratio of the critical impulse  $I$  to  $I_{S.M.}$ , the impulse given by the formula (40) for the simple cubic model, varies with the spectral parameters  $k$  and  $c$ . The frequency used in the simple-model formula was (57), that of the critical buckling mode. Values of this ratio less than unity imply that use of the simple-model formula would be unconservative, and so, as Figure 15 shows, unconservatism is the rule rather than the exception over the  $(k,c)$  domain of imperfection spectra. With hindsight, these results are not implausible; the simple model could be expected to be reliable only if wave numbers in the vicinity of  $\nu = 1$  were predominant in the buckling process. But for high  $k$ , the spectrum given by (60) is relatively flat, and for low  $k$  and high  $c$ , the spectra are peaked near  $\nu = c$ ; evidently, the imperfection spectra strongly influence the subsequent deformation spectra, and so only for low  $k$ , and  $c$  near or less than unity are the simple-model results conservative for impulsive loading.

---

\* If the results are right, mathematically, they imply that a little damping would permit this ideal structure to withstand a step loading greater than  $\lambda_S$  for a while -- but then, as damping gradually eliminated the oscillations, it would buckle statically!

CONCLUDING REMARKS

A general theory of dynamic buckling of imperfection-sensitive elastic structures has been presented. The results obtained therefrom are believed to be widely applicable, but their use must be tempered by careful consideration of the extent to which the basic assumptions of the theory are met. In particular, serious deviations from the results of the general theory could occur when the structure under consideration enjoys a multiplicity of buckling modes near the lowest classical buckling load, and is subjected to impulsive or short-duration loadings.

REFERENCES

- Budiansky, B. and J. W. Hutchinson (1964) Dynamic Buckling of Imperfection-Sensitive Structures, Proc. XI Internat. Cong. Appl. Mech., Munich.
- Fraser, W. B. (1965) Buckling of a Structure with Random Imperfections, Ph.D. Thesis, Harvard University.
- Goodier, J. N. and I. K. McIvor (1964) The Elastic Cylindrical Shell under Nearly Uniform Radial Impulse, J. Appl. Mech., 31, 2.
- Hoff, N. J. and V. G. Bruce (1954) Dynamic Analyses of the Buckling of Laterally Loaded Flat Arches, J. Math. and Physics, 32, 4.
- Humphreys, J. S. (1966) A Note on the Adequacy of Energy Criteria for Dynamic Buckling of Arches, to be published in AIAA Journal.
- Hutchinson, J. W. and B. Budiansky (1966) Dynamic Buckling Estimates, to be published in AIAA Journal.
- Koiter, W. T. (1945) On the Stability of Elastic Equilibrium (in Dutch), Thesis, Delft, H. J. Paris, Amsterdam.
- (1963) Elastic Stability and Post Buckling Behavior, in "Non-Linear Problems", edited by Langer, R. E., Univ. of Wisconsin Press.
- Stoker, J. J. (1950) Nonlinear Vibrations, Interscience, New York.

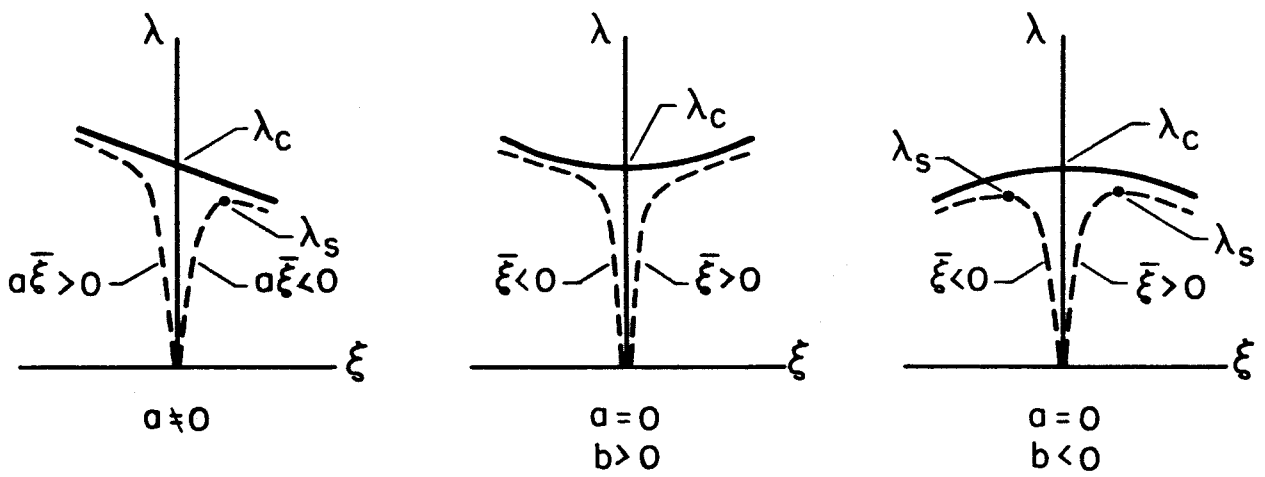


FIG. 1 LOAD-DEFLECTION CURVES



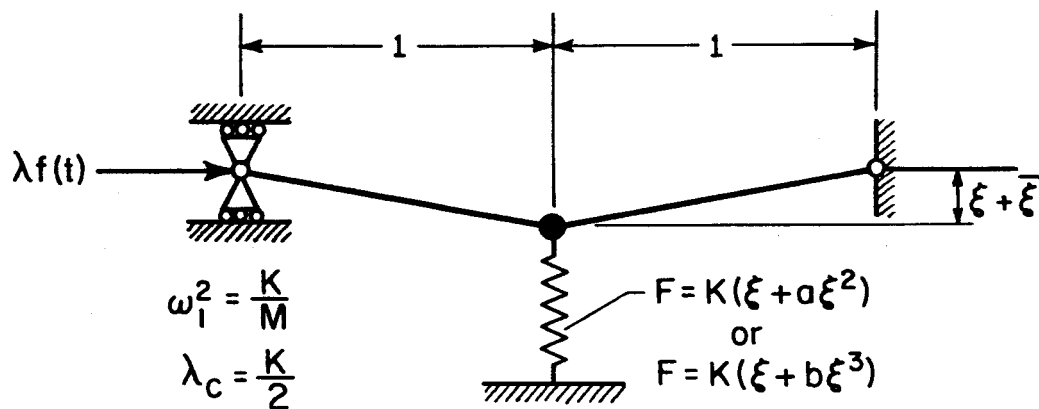


FIG. 2 SIMPLE MODEL

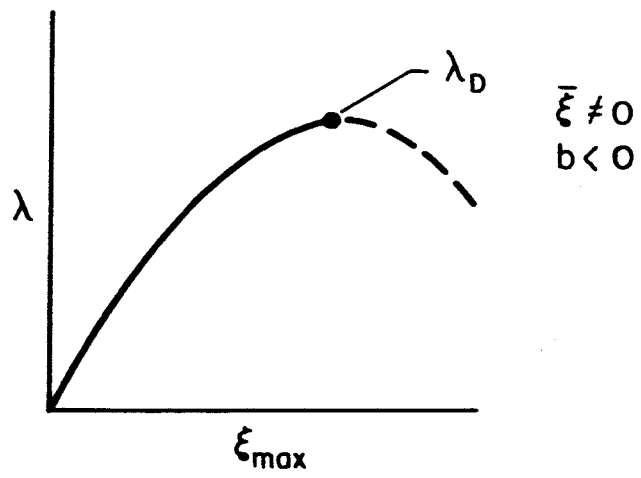


FIG. 3 STEP LOADING OF CUBIC STRUCTURE,  
LOAD VS. MAXIMUM DEFLECTION

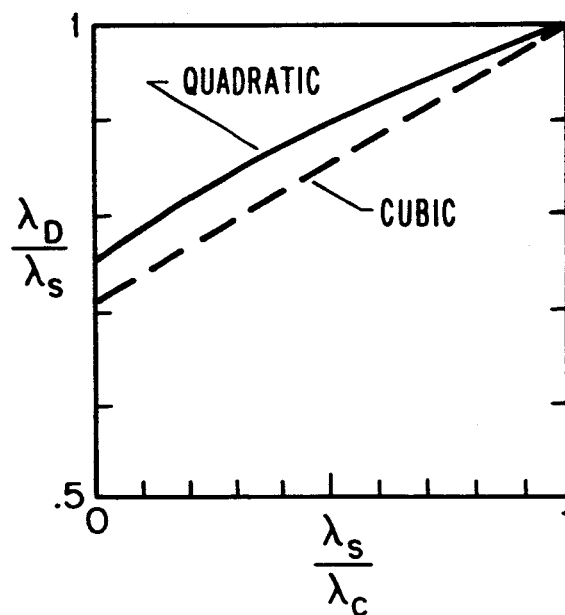


FIG. 4 DYNAMIC BUCKLING, STEP LOADING

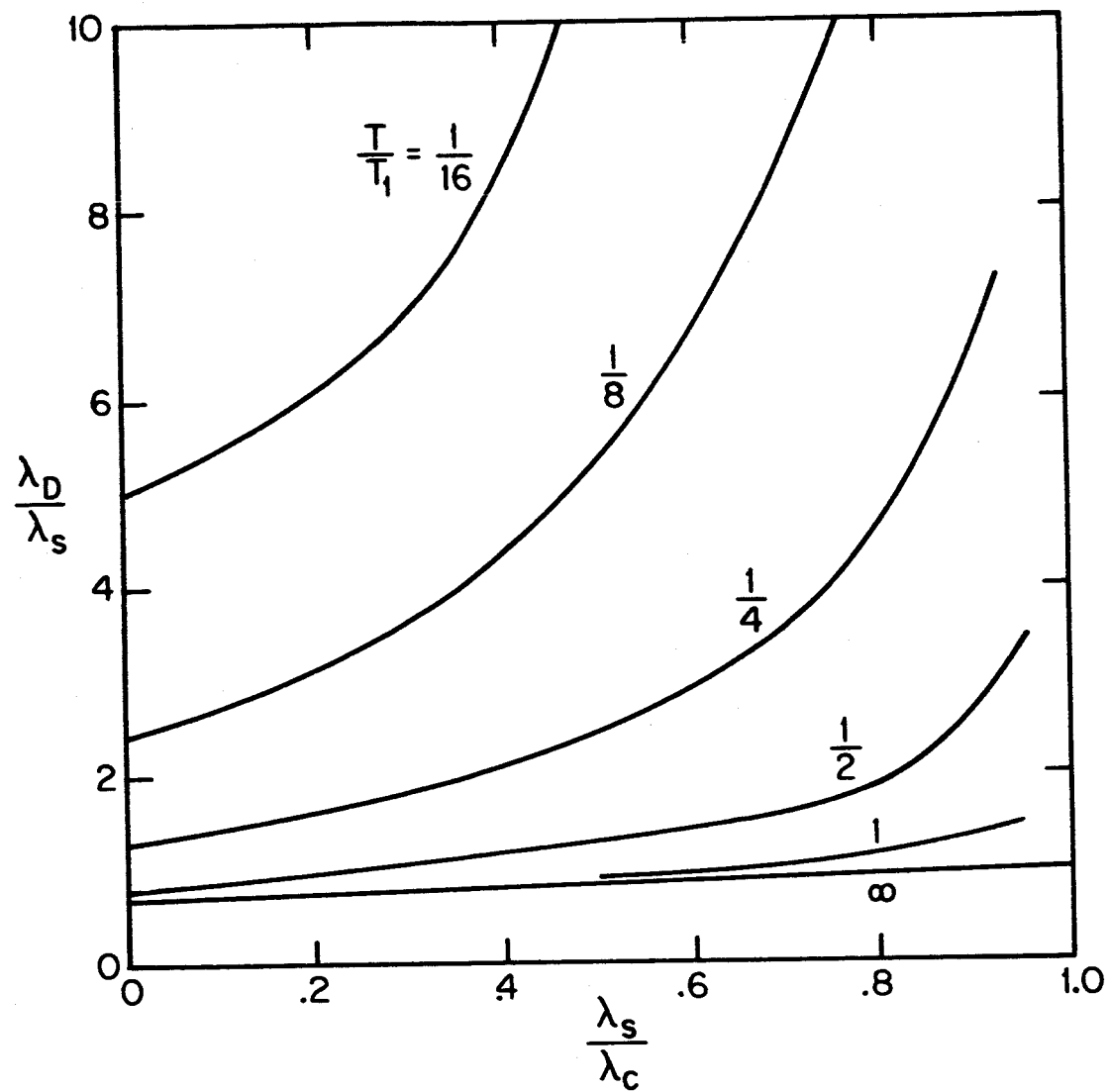


FIG. 5 DYNAMIC BUCKLING, TRANSIENT LOADING  
(CUBIC STRUCTURE)

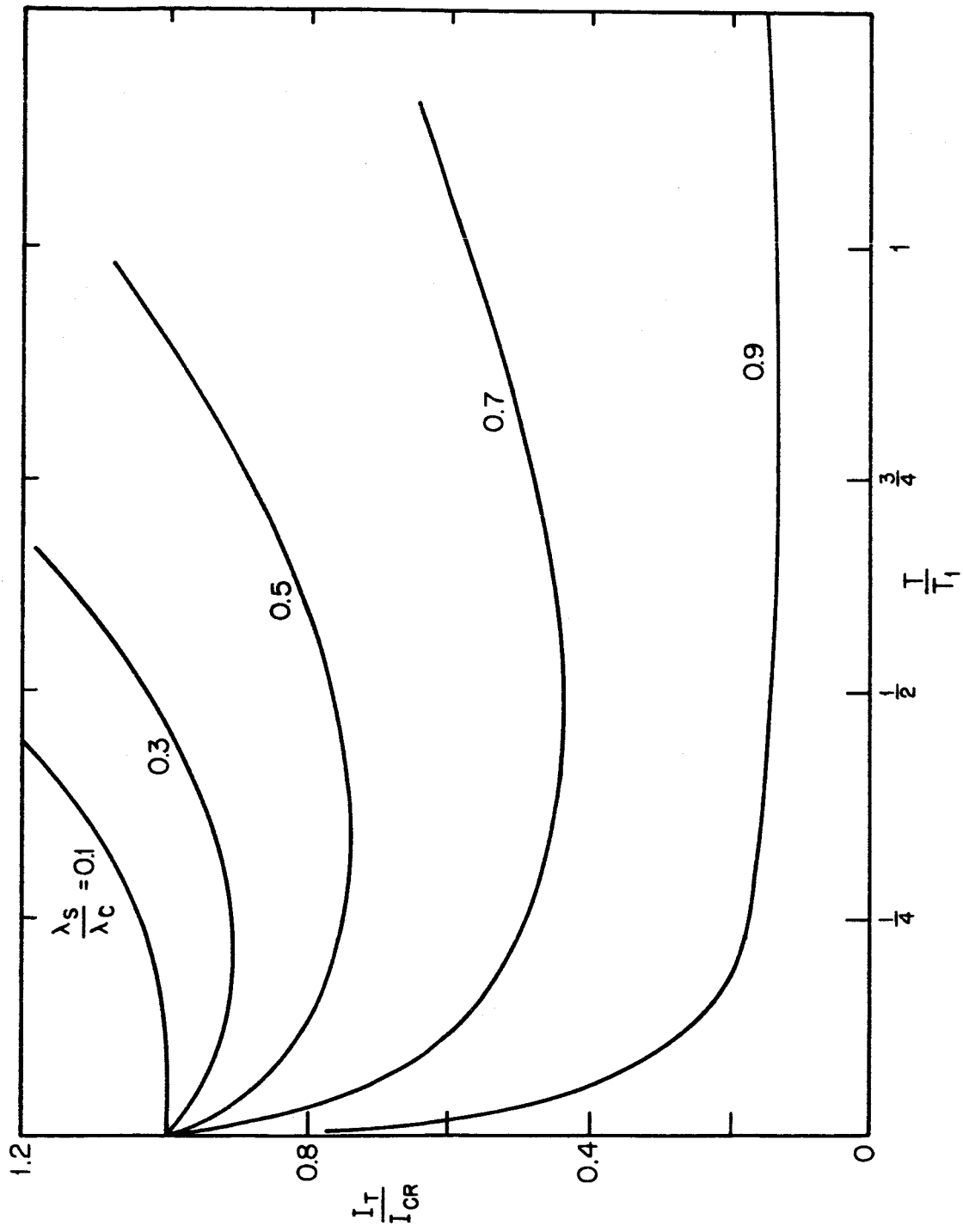


FIG. 6 FINITE-TIME BUCKLING IMPULSE (CUBIC STRUCTURE)

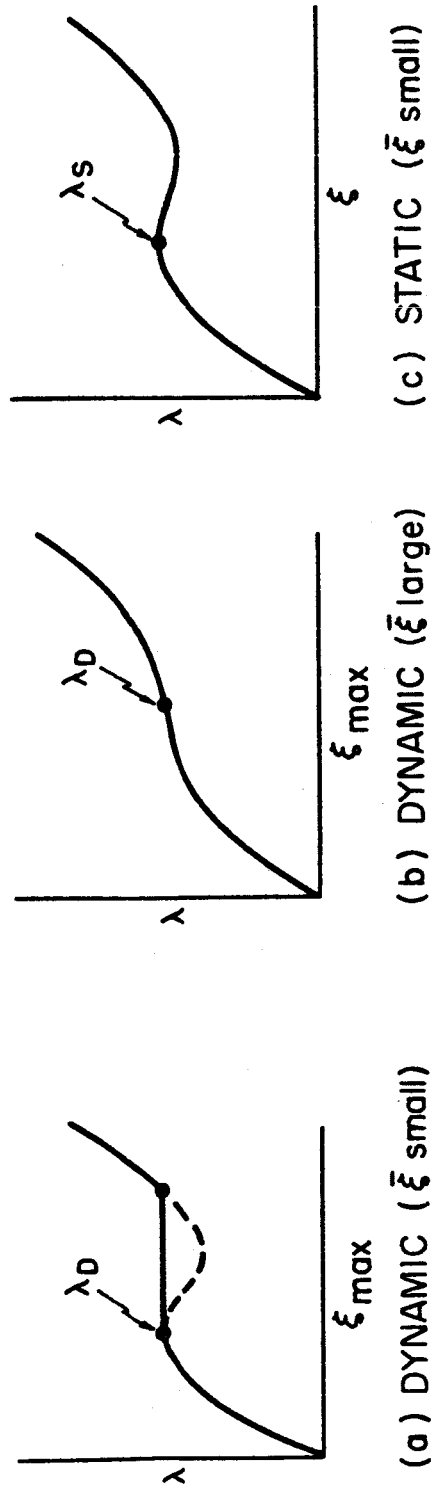


FIG. 7 LOAD vs. RESPONSE, DYNAMIC AND STATIC

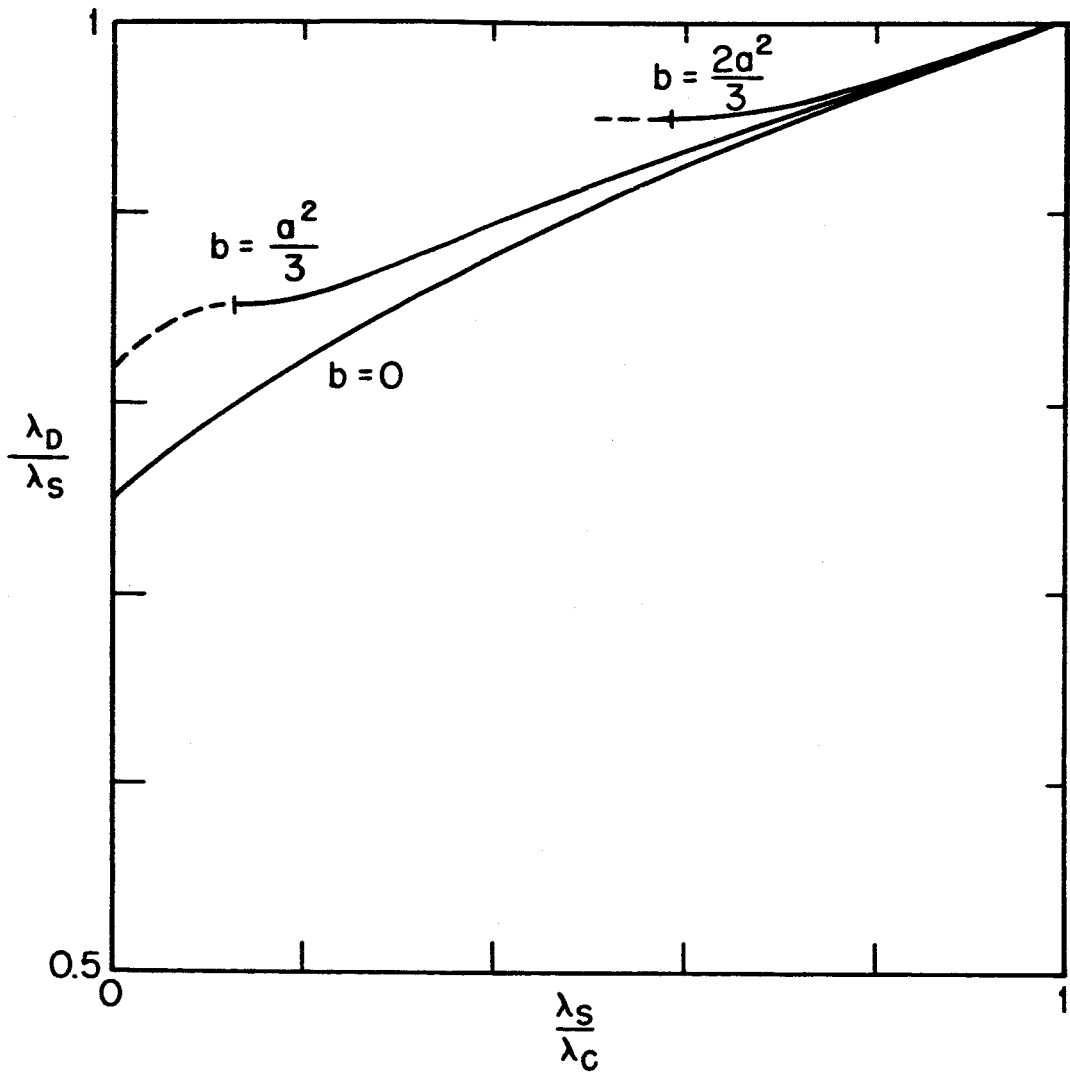


FIG. 8 DYNAMIC BUCKLING, STEP LOADING, QUADRATIC-CUBIC MODEL

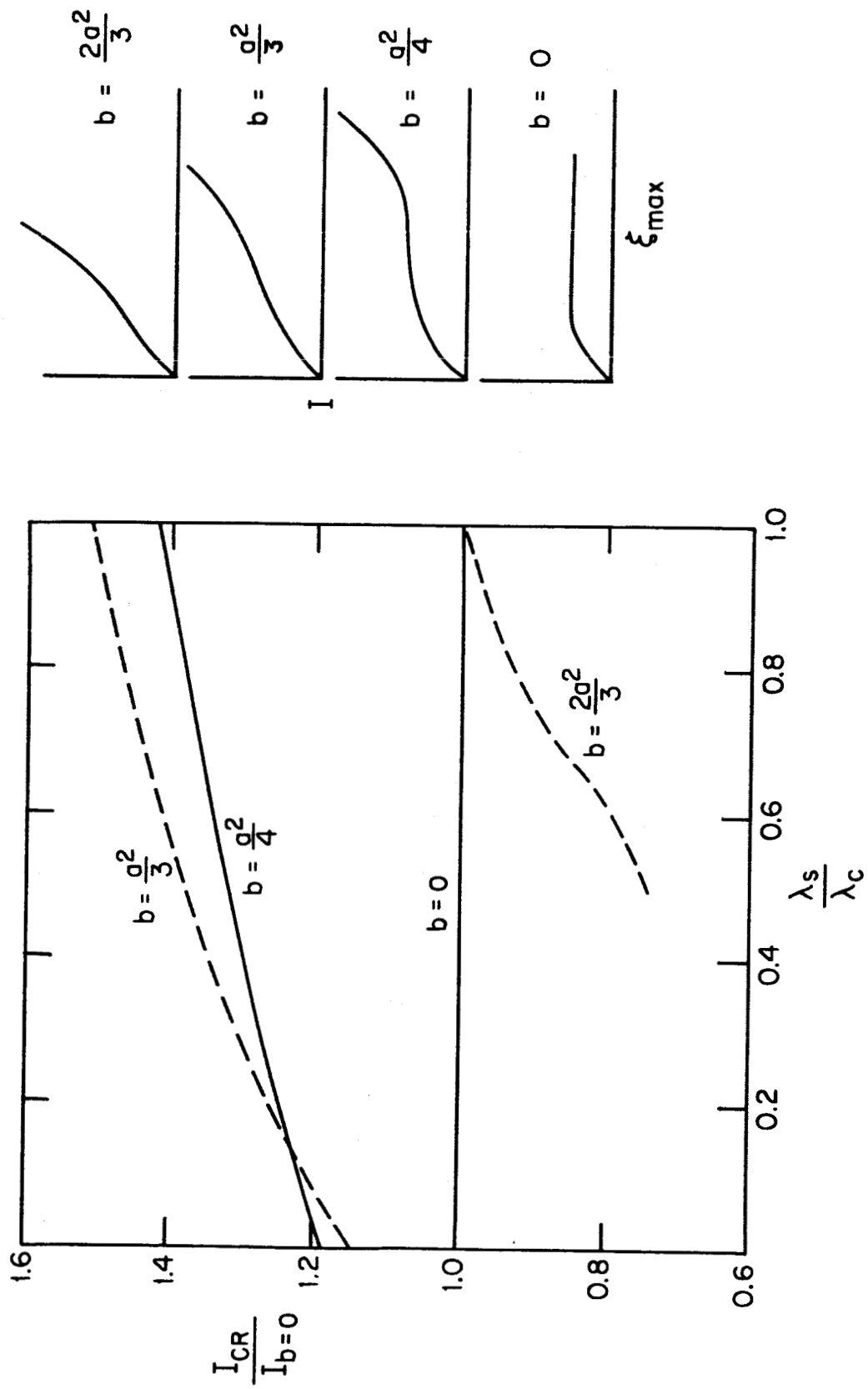
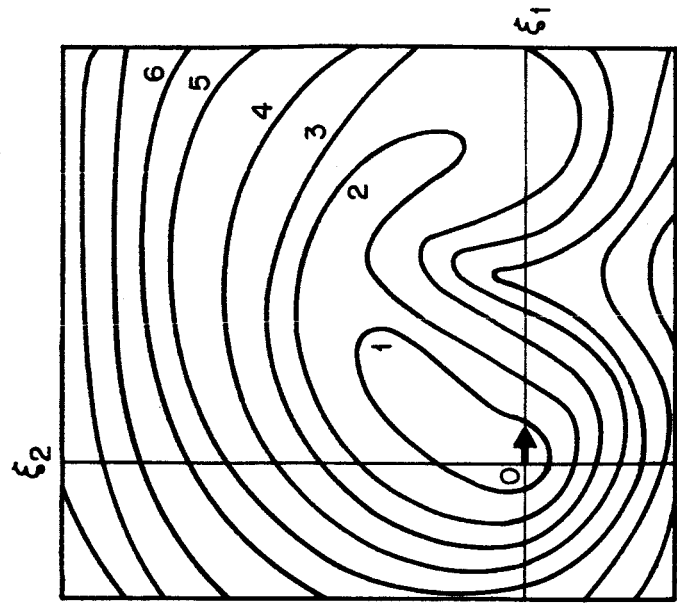
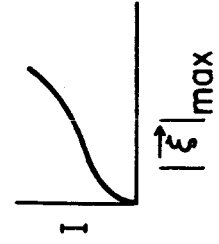


FIG. 9 DYNAMIC BUCKLING, IMPULSIVE LOADING, QUADRATIC-CUBIC MODEL

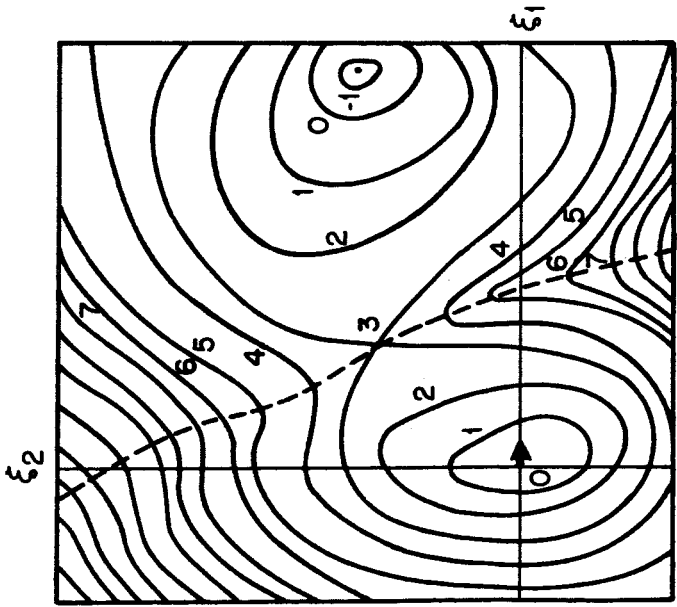




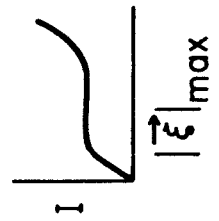
ONE BOWL WITH RIDGE



(b)

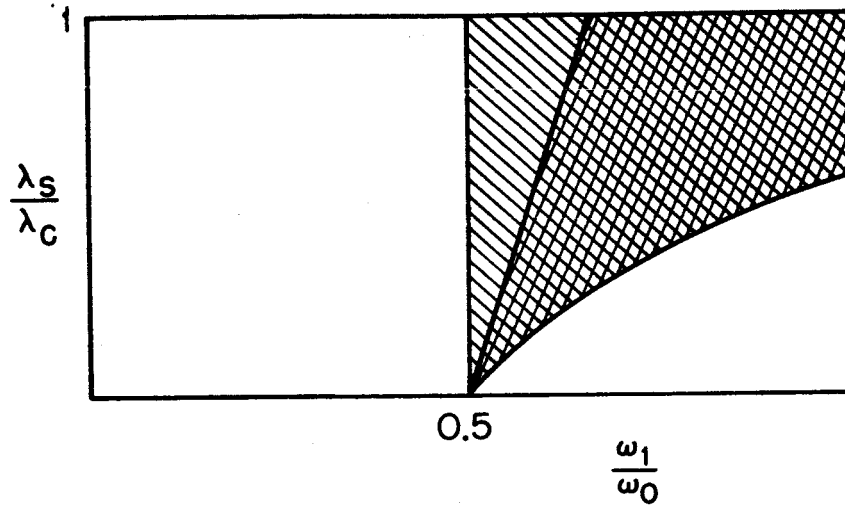


TWO BOWLS



(a)

FIG. 10 TWO CONTOUR PLOTS

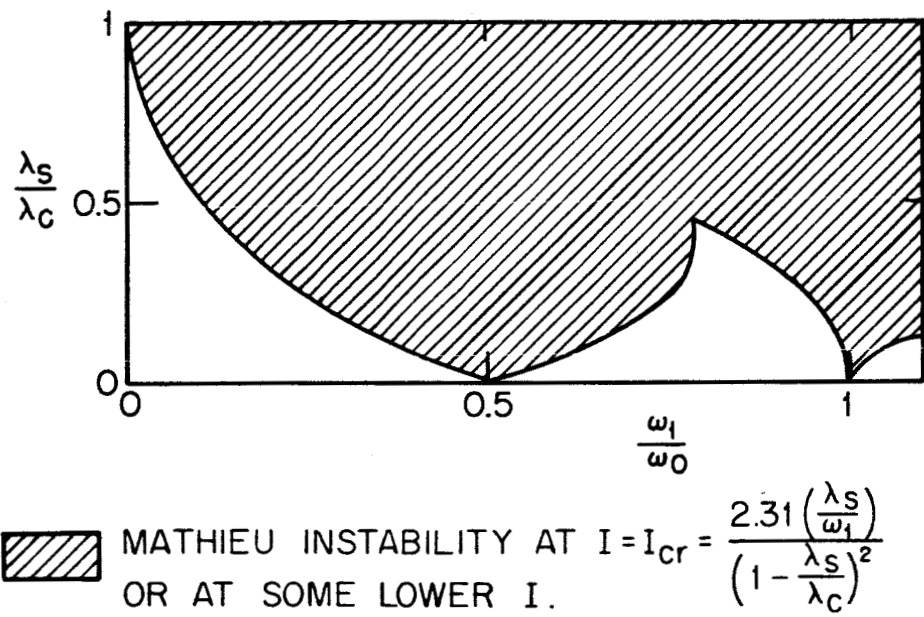


MATHIEU INSTABILITY AT  $\lambda = \lambda_D$

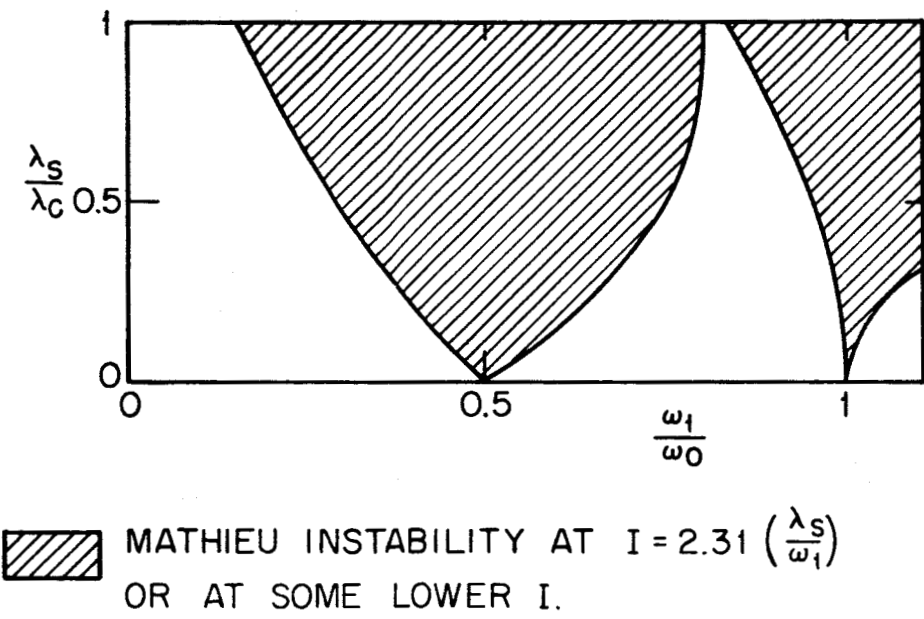


MATHIEU INSTABILITY AT SOME  $\lambda$  LESS THAN  $\lambda_D$

FIG. 11 MATHIEU INSTABILITY, LINEARIZED EQUATIONS, STEP LOADING



(a)



(b)

FIG. 12 MATHIEU INSTABILITY, LINEARIZED EQUATIONS, IMPULSIVE LOADING.

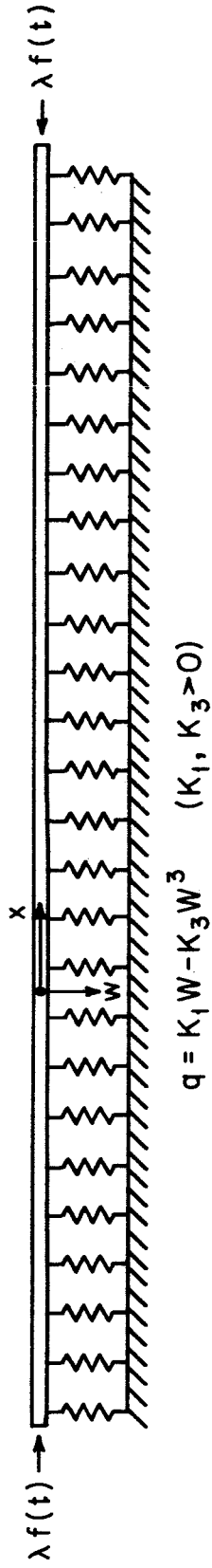


FIG. 13 INFINITELY LONG COLUMN ON A NON-LINEAR FOUNDATION

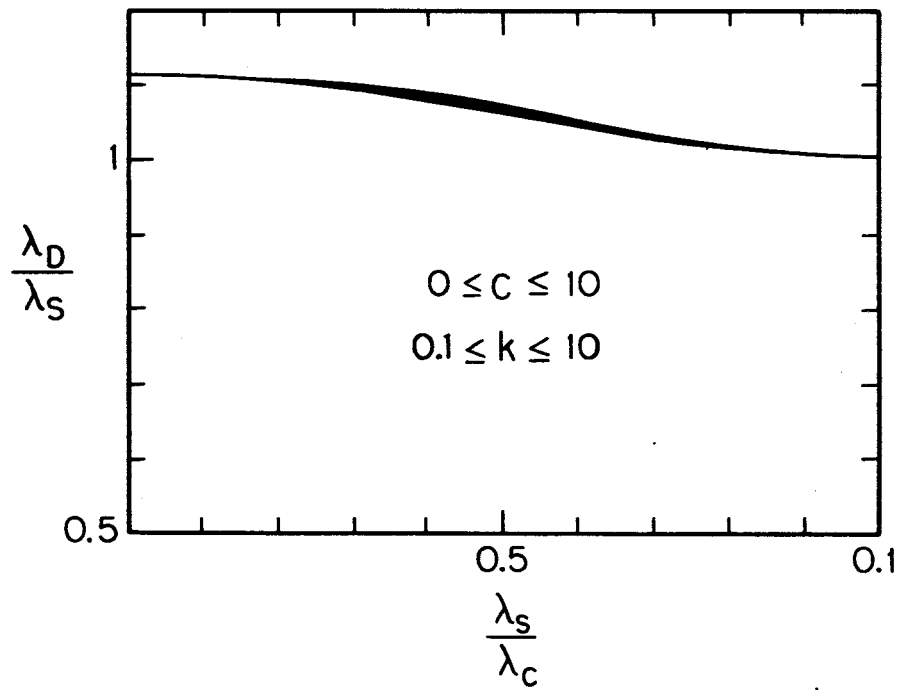


FIG. 14 DYNAMIC BUCKLING, COLUMN WITH RANDOM IMPERFECTIONS, STEP LOADING

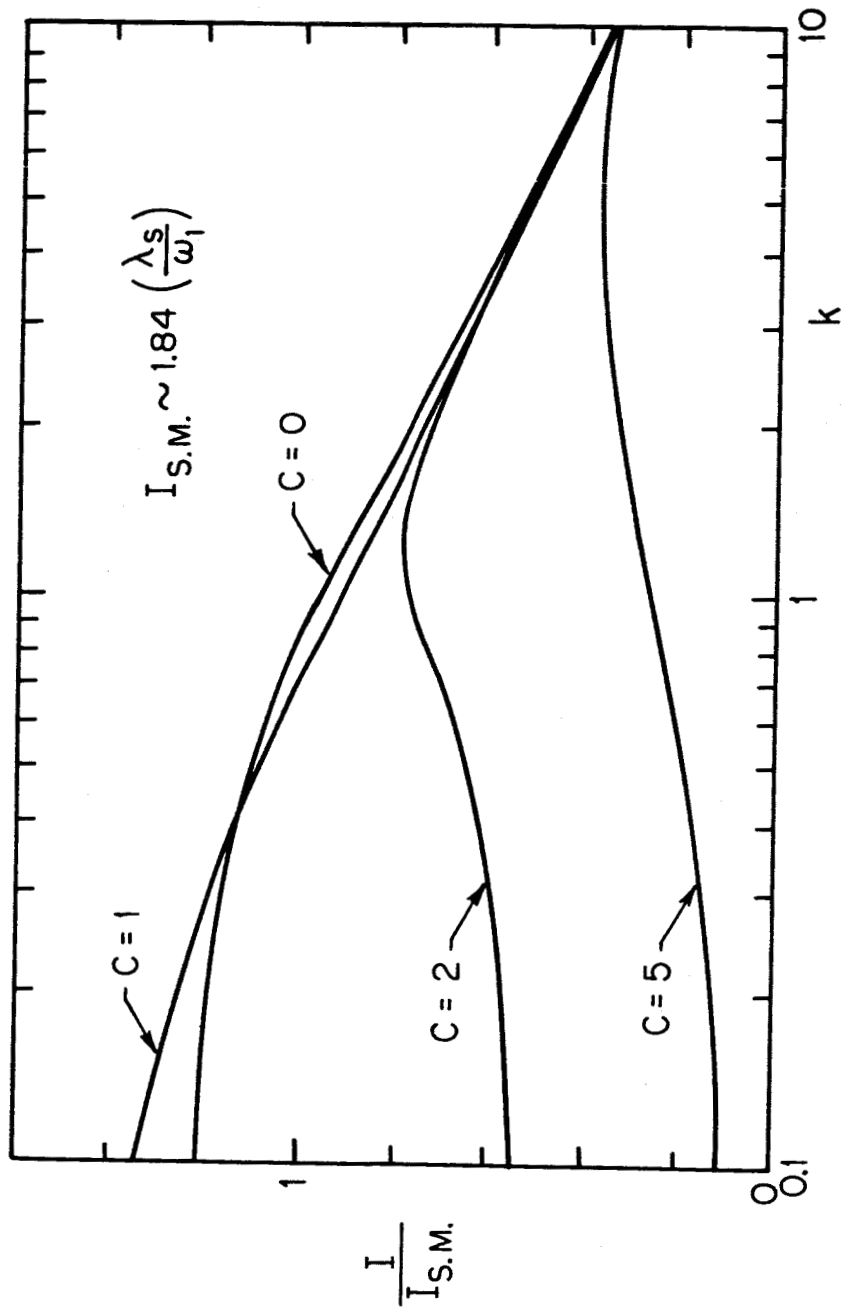


FIG. 15 DYNAMIC BUCKLING, VERY IMPERFECT COLUMN WITH  
RANDOM IMPERFECTIONS, IMPULSIVE LOADING